Photonic Band Structure Computation Using FLAME

Igor Tsukerman and František Čajko

Department of Electrical and Computer Engineering, The University of Akron, OH 44325-3904 USA

The flexible local approximation method (FLAME) is applied for the first time to the computation of the band diagrams of periodic dielectric structures (photonic crystals). Numerical experiments show that FLAME attains high accuracy on fairly coarse grids, with 6–8 orders of magnitude lower errors in the dispersion curves than alternative methods such as finite-element analysis or plane wave expansion with the same number of degrees of freedom.

***Index Terms*—Difference schemes, flexible approximation, photonic band gap, photonic crystals, wave propagation.**

I. Introduction

ARTIFICIAL periodic dielectric structures—"photonic crystals"—with features smaller, but not much smaller, than the wavelength of light can have forbidden frequency bands (the Photonic Band Gap, PBG) [1], [2] and may allow one to control the propagation of light. The PBG/band structure computation is traditionally based on spatial Fourier transforms [plane wave expansion (PWE)]. However, for high dielectric contrasts too many plane waves are needed to achieve reasonable accuracy. A variety of other methods, both in the time and frequency domain, have also been used. These include the finite-element method (FEM) and finite-difference time domain (FDTD)/beam propagation techniques; see, for example, [9], [10] and, for additional references, [4].

The flexible approximation method (FLAME) [3]–[5] has previously been used to simulate wave propagation and waveguide modes in photonic crystals [7]. In the present paper, FLAME is applied, for the first time, to photonic band structure computation. Numerical experiments show that the method converges very rapidly and can lead to 6–8 orders of magnitude higher accuracy than PWE or FEM with a comparable number of degrees of freedom.

II. FLAME Schemes for Photonic Crystals

We consider band structure calculation in a photonic crystal formed by an infinite lattice of cells $L_x \times L_y$ in the xy-plane. In a very common case, each cell contains a dielectric cylindrical rod with a radius $r_{\rm rod}$ and the relative dielectric permittivity $\epsilon_{\rm rod}$ (Fig. 1). The medium outside the rod has permittivity $\epsilon_{\rm out}$. All media are nonmagnetic.

The E-mode (one component of the electric field $E = E_z$) is governed by the wave equation

$$\nabla^2 E + \omega^2 \mu_0 \epsilon E = 0 \tag{1}$$

where $\epsilon = \epsilon(x, y)$. The E field is sought as a Bloch-Floquet wave [8] with a (yet undetermined) Bloch vector $\mathbf{K}_B$

$$E(\mathbf{r}) = E_{\rm PER}(\mathbf{r}) \exp(-\mathrm{i}\mathbf{K}_B \cdot \mathbf{r}) \quad \mathbf{r} \equiv (x, y). \tag{2}$$

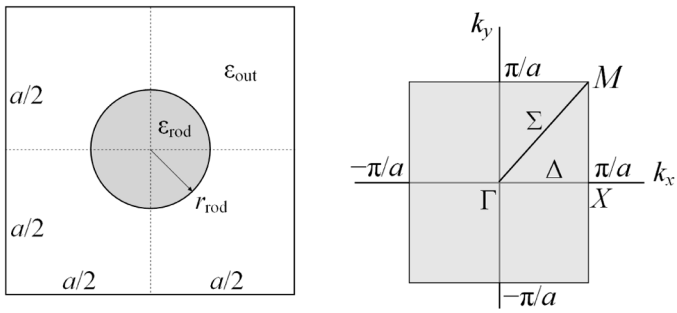

Fig. 1. (Left) Square cell of a photonic crystal lattice. The crystal is obtained by periodic replication of the cell in both coordinate directions. (Right) The first Brillouin zone and special points Γ, X, M in reciprocal space.

In the space of Bloch vectors $\mathbf{K}_B$, the "master" cell $[-\pi/L_x, \pi/L_x] \times [-\pi/L_y, \pi/L_y]$ is called the first *Brillouin zone* (Fig. 1). For notational simplicity and without any real loss of generality, we shall frequently refer to a square lattice cell with $L_x = L_y = a$.

The standard notation for some special points in the Brillouin zone is as follows. The Γ point $\mathbf{K}_B = 0$ corresponds to the purely periodic field $E_{\rm PER}$ in both x and y directions. The X point $\mathbf{K}_B = [\pi L_x^{-1}, 0]$ describes the Bloch wave propagating in the x-direction. The M point $\mathbf{K}_B = [\pi L_x^{-1}, \pi L_y^{-1}]$ corresponds to the Bloch wave traveling, for a square lattice cell, at the 45° angle to the x- and y-axes.

Three methods are compared below: PWE, FEM, and FLAME. The gist of FLAME is in replacing the Taylor polynomials of classical FD analysis with accurate local analytical approximations, which in many cases substantially improves the quality of the numerical solution. In particular, in the vicinity of a cylindrical rod centered at the origin of a polar coordinate system (r, ϕ), the FLAME basis $\psi_\alpha^{(i)}$ contains Bessel/Hankel functions [3]–[5]

$$\psi_\alpha^{(i)} = a_n J_n(k_{\rm cyl} r) \exp(\mathrm{i}n\phi), \quad r \le r_{\rm rod}$$
$$\psi_\alpha^{(i)} = \left[c_n J_n(k_{\rm air} r) + H_n^{(2)}(k_{\rm air} r)\right] \exp(\mathrm{i}n\phi), \qquad r > r_{\rm rod}$$

where J_n is the Bessel function, $H_n^{(2)}$ is the Hankel function of the second kind [11], and a_n, c_n are coefficients to be determined. These coefficients are found via the standard conditions on the boundary of the cylinder; see [3]–[5] for further details. Index i runs over all grid stencils where the FLAME

Digital Object Identifier 10.1109/TMAG.2007.916166

Color versions of one or more of the figures in this paper are available online at http://ieeexplore.ieee.org.

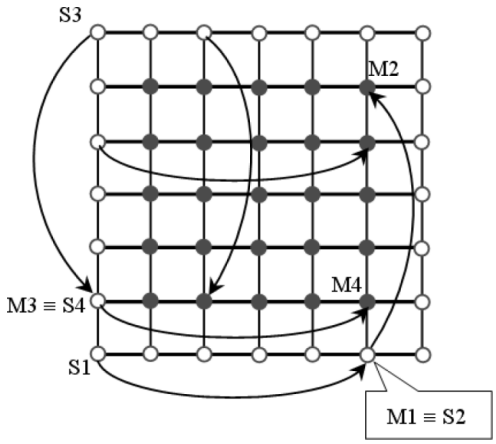

Fig. 2. Implementation of the Bloch-Floquet boundary conditions in FLAME. Empty circles—"slave" nodes, filled circles—"master" nodes. A few of the "slave-master" links are indicated with arrows. The corner nodes are the "slaves of slaves."

scheme is generated, while index α runs over all basis functions in stencil i.

In this paper, the nine-point (3×3) stencil with a grid size h is used and $1 \leq \alpha \leq 8$. The eight basis functions ψ are obtained by retaining the monopole harmonic $(n = 0)$, two harmonics of orders $n = 1, 2, 3$ (i.e., dipole, quadrupole and octupole), and one of harmonics of order $n = 4$. This set of basis functions produces a nine-point scheme as the null vector of the respective matrix of nodal values [3]–[5].

The Bloch wave satisfying the second-order differential equation calls for *two* boundary conditions—for the E field and for its derivative in the direction of wave propagation (or, equivalently, for the H field). Consequently, there are two discrete boundary conditions per Cartesian coordinate (compare this with a similar treatment in [7] where, however, the algorithm is effectively 1-D). The implementation of these discrete conditions is illustrated by Fig. 2, where the square lattice cell is covered with a 5×5 grid of "master" nodes (filled circles). In addition, there is a border layer of "slave" nodes (empty circles).

The FLAME scheme is generated for each of the *master nodes* ("M"). At slave nodes ("S"), the field is constrained by the Bloch-Floquet condition rather than by the difference scheme

$$E(\mathbf{r}_S) = \exp\left(-\mathrm{i}\mathbf{K}_B \cdot (\mathbf{r}_S - \mathbf{r}_M)\right) E(\mathbf{r}_M). \tag{3}$$

Here $\mathbf{r}_S$, $\mathbf{r}_M$ are the position vectors of any given slave-master pair of nodes. Several such pairs are indicated in Fig. 2 by the arrows for illustration. Note that the corner nodes are the "slaves of slaves": for example, master node M1 for slave S1 is itself a slave S2 of node M2. This is algebraically equivalent to linking node S1 to M2; however, if the link $S1 \rightarrow M2$ were imposed directly rather than via $S1 \rightarrow M1 \rightarrow M2$, the corresponding factor would be the product of two Bloch exponentials in the x- and y-direction, leading to a complicated eigenvalue problem, bilinear with respect to both exponentials.

Example equations for the Bloch boundary conditions, in reference to Fig. 2, are

$$E_{\mathrm{S1}} = b_x E_{\mathrm{M1}} \qquad b_y E_{\mathrm{S3}} = E_{\mathrm{M3}} \tag{4}$$

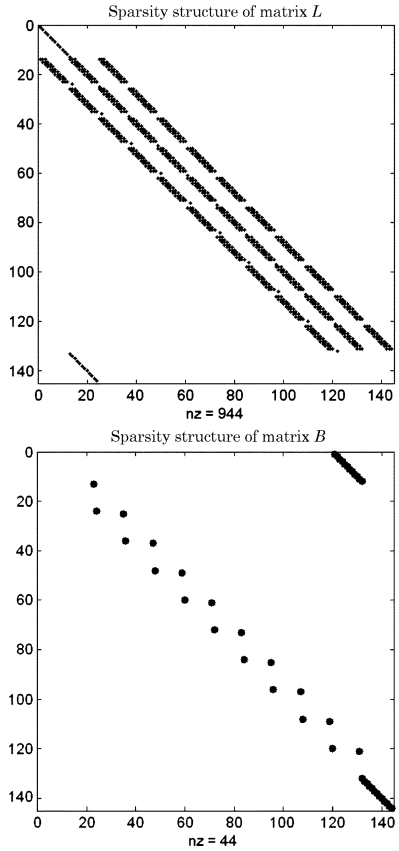

Fig. 3. Sparsity structure of the FLAME matrices for a 10×10 grid: L (top, 944 nonzero entries) and $B = B_x + B_y$ (bottom, 44 nonzero entries).

where b_x and b_y are the Bloch factors

$$b_x = \exp(\mathrm{i}K_x L_x) \qquad b_y = \exp(\mathrm{i}K_y L_y). \tag{5}$$

In matrix-vector form, the FLAME eigenvalue problem is

$$L\underline{E} = (b_x B_x + b_y B_y)\underline{E} \tag{6}$$

where $\underline{E}$ is the Euclidean vector of nodal values of the field. The rows of matrix L corresponding to the master nodes contain the coefficients of the FLAME scheme, and the respective rows of matrices $B_{x,y}$ are zero. Each slave-node row of matrices L and B contains only one nonzero entry—either 1 or $b_{x,y}$, as exemplified by (4). Matrices L and (especially) B are sparse; typical sparsity patterns, for a 10×10 grid, are shown in Fig. 3.

Problem (6) contains three key parameters: ω, on which the FLAME scheme and hence the L matrix depend (for brevity, this dependence is not explicitly indicated), and the Bloch exponentials $b_{x,y}$. Finding three or even two independent eigenparameters simultaneously is not feasible. First, one chooses a value of ω and constructs the difference operator L for that value. In principle, for any given value of either of the b parameters (say, b_x) one could solve for the other parameter and scan the (b_x, b_y)-plane that way. This is usually not necessary, however, as the focus is typically on the symmetry lines $\Gamma \rightarrow X \rightarrow M \rightarrow \Gamma$ of the first Brillouin zone. On ΓX, $b_y = 1$ and b_x is the only unknown; on XM, the only unknown is b_y; and on $M\Gamma$, the single unknown is $b = b_x = b_y$.

III. Band Structure Computation Using Plane Wave Expansion

PWE is a Fourier transform method extensively covered in the literature (e.g., [8], among many others). In this paper, PWE will only be used as a point of comparison with FLAME, so a very brief description will suffice.

In Fourier space, $E_{\rm PER}$ is given by its Fourier series with coefficients $e_{\mathbf{m}}$ ($\mathbf{m} = (m_x, m_y)$; $m_x, m_y = 0, \pm 1, \pm 2, \ldots$)

$$E(\mathbf{r}) = \sum_{\mathbf{m}\in\mathbb{Z}^2} e_{\mathbf{m}} \exp(\mathrm{i}\kappa_0 \mathbf{m}\cdot\mathbf{r}) \exp(-\mathrm{i}\mathbf{K}_B\cdot\mathbf{r}) \tag{7}$$

where $\kappa_0 = 2\pi a^{-1}$. The periodic permittivity ϵ is expressed via a Fourier series with coefficients $\epsilon_{\mathbf{m}}$

$$\epsilon(\mathbf{r}) = \sum_{\mathbf{m}\in\mathbb{Z}^2} \epsilon_{\mathbf{m}} \exp(\mathrm{i}\kappa_0 \mathbf{m}\cdot\mathbf{r}). \tag{8}$$

The Fourier transform of the wave equation (1) converts multiplication ϵE into convolution and the Laplace operator—into multiplication by $-|\mathbf{K}_B - \kappa_0\mathbf{m}|^2$. In matrix form

$$\mathcal{K}^2 \underline{e} = \omega^2 \mu_0 \Xi \underline{e} \tag{9}$$

where $\underline{e} = (\ldots, e_{-2}, e_{-1}, e_0, e_1, e_2, \ldots)^T$ is the (infinite) column vector of Fourier coefficients; $\mathcal{K}^2$ is an infinite diagonal matrix with the entries

$$(\mathcal{K}^2)_m = |\mathbf{K}_B - \kappa_0\mathbf{m}|^2 \tag{10}$$

and matrix Ξ is composed of the Fourier coefficients of ϵ

$$\Xi_{ml} = \epsilon_{m-l} \tag{11}$$

for any row m and column l ($-\infty < m, l < \infty$).

The infinite-dimensional eigenproblem (9) must in practice be truncated to a finite number of harmonics. As the number of harmonics retained in the system grows, both computational complexity and accuracy increase.

IV. Band Structure Computation Using FEM

Like PWE, in this paper FEM plays an auxiliary role of providing a comparison case for FLAME. As the essence of the method is very well known (see especially [6]), only a brief summary is given here.

There are two general options for FEM: solving for the full E-field of (1) as done in this paper or, alternatively, for the periodic factor $E_{\rm PER}(x, y)$ as done in [6]. In the first case, the governing equation is fairly simple (Helmholtz), but the boundary conditions are nonstandard due to the Bloch exponential $\exp(-\mathrm{i}\mathbf{K}_B\cdot\mathbf{r})$. In the second case, with $E_{\rm PER}$ as the unknown, standard periodic boundary conditions apply, but the differential operator is more complicated [4], [6].

In both cases, the eigenvalue problems are unusual, as they have three scalar eigenparameters: frequency ω and the components K_x, K_y of the Bloch vector. As in FLAME, solving for these three parameters, and the respective eigenmodes, simultaneously is impractical. But in contrast with FLAME, where ω needs to be fixed first to generate the scheme, in PWE and FEM the usual approach is to choose the $\mathbf{K}_B$ vector first and then solve the resultant eigenvalue problem for ω; the computation is repeated for a desired set of values of $\mathbf{K}_B$.

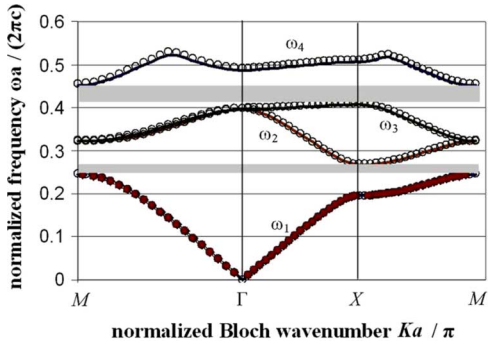

Fig. 4. Photonic band structure (first four eigenfrequencies as a function of the wavevector) for a photonic crystal lattice. FEM (circles), PWE (solid lines), FLAME, grid 5×5 (diamonds), FLAME, grid 20×20 (squares). Dielectric cylindrical rods in air; cell size $a = 1$, radius of the cylinder $r_{\rm rod} = 0.38$; the relative dielectric permittivities $\epsilon_{\rm rod} = 9$; $\epsilon_{\rm out} = 1$.

A natural functional space for the problem is the subspace of "scaled-periodic" functions in the Sobolev space $H^1(\Omega)$. The weak formulation is obtained in the standard integration-by-parts way, and it can be easily verified that the boundary integrals vanish and do not appear in the formulation.

The handling of the Bloch boundary conditions in FEM is also straightforward if the opposite edges of the computational domain Ω are subdivided by the grid nodes in an identical fashion, so that the nodes come in master-slave pairs. (For *edge elements*, one would consider pairs of master-slave *edges* rather than nodes.) The end result of the FE discretization is an eigenvalue problem of the form

$$L\underline{E} = \omega^2 \mu_0 M \underline{E}.$$

Matrices L and M are the FE "stiffness" and "mass" matrices, respectively. Their entries can be written out explicitly

$$L_{\alpha\beta} = (\nabla\psi_\alpha, \nabla\psi_\beta) \quad 1 \le \alpha, \beta \le n \tag{12}$$

$$M_{\alpha\beta} = (\epsilon\psi_\alpha, \psi_\beta) \quad 1 \le \alpha, \beta \le n \tag{13}$$

where the inner products are those of $L_2(\Omega)$ and the ψ's are the FE basis functions. Matrices L, M are Hermitian; the stiffness matrix L is positive definite if the Bloch wavenumber K_B is nonzero; the mass matrix M is always positive definite.

V. Numerical Results

For comparison purposes, the numerical data were chosen the same as in the PWE example in [8, pp. 28–29]. In the lattice of cylindrical rods, the size of the computational square cell is $a = 1$, and the radius of the cylindrical rod is $r_{\rm rod} = 0.38$. The dielectric constant of the rod is $\epsilon_{\rm rod} = 9$; the medium outside the rod is air, with $\epsilon_{\rm out} = 1$. In our FLAME simulation, due to very rapid convergence of the method, matrices L and M need only be of very moderate size and the Matlab QZ algorithm (a direct solver for generalized eigenvalue problems) is employed.

Fig. 4 shows the first four normalized eigenfrequencies $\omega a/(2\pi c)$ (c being the speed of light in free space) versus the normalized Bloch wavenumber Ka/π over the

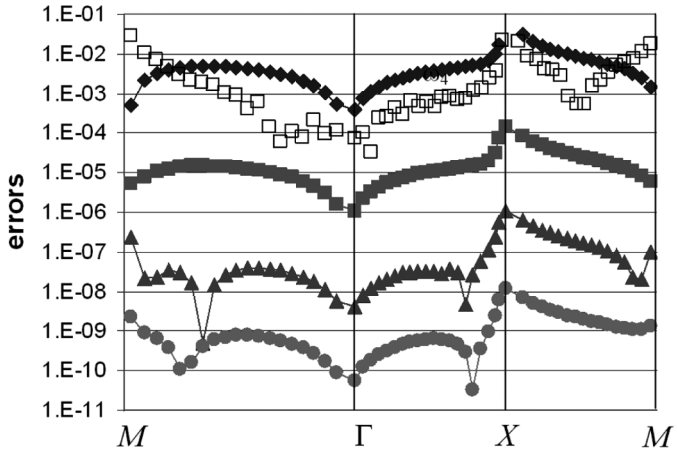

Fig. 5. Numerical errors in the Bloch wavenumber. FLAME grids: 5×5 (diamonds), 8×8 (squares), 10×10 (triangles), 20×20 (circles). FEM, 404 degrees of freedom (empty squares).

$M \to \Gamma \to X \to M$ loop in the Brillouin zone. The bandgaps, where no (real) eigenfrequencies exist for *any* $\mathbf{K}_B$, are shaded in the figure. The excellent agreement between PWE, FEM, and FLAME gives us full confidence in these results and allows us to proceed to a more detailed assessment of the numerical errors.[1]

On an FE mesh with 1553 degrees of freedom (2984 first-order elements), the first two frequency bandgaps are calculated to be [0.2457, 0.2678] and [0.4081, 0.4527]. This differs from the results on a coarser mesh with 404 degrees of freedom and 746 elements by 0.2–0.7%.

The first bandgap is obtained with the estimated accuracy of $\sim$0.5% on the finer FE mesh and of $\sim$1% for PWE with 441 waves. For comparison, the first two bandgap frequency ranges reported for the same problem by Sakoda [8] are [0.247, 0.277] and [0.415, 0.466] (also with 441 plane waves). Sakoda estimated the error to be about 1%.

The accuracy of FLAME is much higher, with negligible errors achieved already for a 10×10 grid. Indeed, inspecting the computed Bloch-Floquet wavenumbers as the FLAME grid size decreases, we observe that 6–8 digits in the result stabilize once the grid exceeds 10×10 and 8–10 digits stabilize once the grid exceeds 20×20. This clearly establishes the 40×40 results as an "overkill" solution that can be taken as quasi-exact for the purpose of error analysis.

Errors in the Bloch wavenumber are plotted in Fig. 5. Very rapid convergence of FLAME with respect to the number of grid nodes is obvious from the figure. Further, the FLAME error for the Bloch number is about six orders of magnitude lower than the FEM error for approximately the same number of unknowns: 484 nodes (including "slaves") in FLAME and 404 nodes in FEM.

[1]All numerical results were also checked for consistency on several meshes and for an increasing number of PWE terms.

VI. Conclusion

FLAME is a promising and effective approach for the computation of photonic band diagrams. In the numerical example involving a lattice of dielectric cylindrical rods, FLAME provides 6–8 orders of magnitude higher accuracy of the photonic band diagram than PWE or FEM with the same number of degrees of freedom ($\sim$400).

To apply FLAME to more general shapes of dielectric structures, one needs accurate local approximations of the theoretical solution. This can be achieved, for example, by approximating the air-dielectric boundaries with arcs in a piecewise fashion and then using the Bessel-Hankel basis described in the paper. Alternatively, basis functions can be obtained as accurate FE solutions of local problems that are much smaller than the global one [12].

Extensions of the methodology to 3-D are also possible, with FLAME basis functions at (piecewise-)spherical boundaries derived from Mie theory. Techniques of this type are currently under investigation (J. Webb, private communication).

Acknowledgment

The work was supported in part by the National Science Foundation NIRT Research Award 0304453.

References

[1] V. P. Bykov, "Spontaneous emission in a periodic structure," *Soviet Physics (J. Exp. Theoret. Phys.)*, vol. 35, no. 2, pp. 269–273, 1972.

[2] E. Yablonovitch, "Inhibited spontaneous emission in solid-state physics and electronics," *Phys. Rev. Lett.*, vol. 58, no. 20, pp. 2059–2062, 1987.

[3] I. Tsukerman, "Electromagnetic applications of a new finite-difference calculus," *IEEE Trans. Magn.*, vol. 41, no. 7, pp. 2206–2225, 2005.

[4] I. Tsukerman, *Computational Methods for Nanoscale Applications: Particles, Plasmons and Waves*. New York: Springer, 2007.

[5] I. Tsukerman, "A class of difference schemes with flexible local approximation," *J. Comput. Phys.*, vol. 211, no. 2, pp. 659–699, 2006.

[6] D. C. Dobson and J. E. Pasciak, "Analysis of an algorithm for computing electromagnetic Bloch modes using Nedelec spaces," *Comput. Meth. Appl. Math.*, vol. 1, no. 2, pp. 138–153, 2001.

[7] H. Pinheiro, J. P. Webb, and I. Tsukerman, "Flexible local approximation models for wave scattering in photonic crystal devices," *IEEE Trans. Magn.*, vol. 43, no. 4, pp. 1321–1324.

[8] K. Sakoda, *Optical Properties of Photonic Crystals*. New York: Springer, 2005.

[9] V. F. Rodriguez-Esquerre, M. Koshiba, and H. E. Hernandez-Figueroa, "Finite-element time-domain analysis of 2-D photonic crystal resonant cavities," *IEEE Photon. Technol. Lett.*, vol. 16, no. 3, pp. 816–818, 2004.

[10] T. Fujisawa and M. Koshiba, "Time-domain beam propagation method for nonlinear optical propagation analysis and its application to photonic crystal circuits," *J. Lightw. Technol.*, vol. 22, no. 2, pp. 684–691, 2004.

[11] R. F. Harrington, *Time-Harmonic Electromagnetic Fields*. Piscataway, NJ: Wiley-IEEE Press, 2001.

[12] J. Dai and I. Tsukerman, "Flexible difference schemes with numerical bases for electrostatic particle interactions," in *Proc. CEFC 2006*, Miami, FL.

Manuscript received June 24, 2007. Corresponding author: I. Tsukerman (e-mail: igor@uakron.edu).